Search for $B^+ \to D^{*+}\pi^0$ Decay

M. Iwabuchi,[4] M. Nakao,[7] I. Adachi,[7] K. Arinstein,[1] V. Aulchenko,[1] T. Aushev,[16,11] A. M. Bakich,[36] V. Balagura,[11] E. Barberio,[19] A. Bay,[16] K. Belous,[10] V. Bhardwaj,[31] U. Bitenc,[12] A. Bozek,[25] M. Bračko,[18,12] T. E. Browder,[6] A. Chen,[22] W. T. Chen,[22] B. G. Cheon,[5] I.-S. Cho,[45] Y. Choi,[35] J. Dalseno,[7] M. Dash,[44] A. Drutskoy,[3] S. Eidelman,[1] M. Fujikawa,[21] N. Gabyshev,[1] H. Ha,[14] J. Haba,[7] K. Hayasaka,[20] M. Hazumi,[7] D. Heffernan,[30] Y. Horii,[39] Y. Hoshi,[38] W.-S. Hou,[24] H. J. Hyun,[15] K. Inami,[20] A. Ishikawa,[32] H. Ishino,[41] R. Itoh,[7] M. Iwasaki,[40] D. H. Kah,[15] H. Kaji,[20] J. H. Kang,[45] H. Kawai,[2] T. Kawasaki,[27] H. Kichimi,[7] H. J. Kim,[15] H. O. Kim,[15] Y. I. Kim,[15] Y. J. Kim,[4] K. Kinoshita,[3] S. Korpar,[18,12] P. Križan,[17,12] P. Krokovny,[7] R. Kumar,[31] C. C. Kuo,[22] Y.-J. Kwon,[45] J. S. Lee,[35] M. J. Lee,[34] S. E. Lee,[34] T. Lesiak,[25] A. Limosani,[19] S.-W. Lin,[24] C. Liu,[33] Y. Liu,[4] D. Liventsev,[11] F. Mandl,[9] A. Matyja,[25] S. McOnie,[36] T. Medvedeva,[11] K. Miyabayashi,[21] H. Miyake,[30] H. Miyata,[27] Y. Miyazaki,[20] G. R. Moloney,[19] H. Nakazawa,[22] Z. Natkaniec,[25] S. Nishida,[7] O. Nitoh,[43] S. Ogawa,[37] T. Ohshima,[20] S. Okuno,[13] H. Ozaki,[7] P. Pakhlov,[11] G. Pakhlova,[11] C. W. Park,[35] H. K. Park,[15] K. S. Park,[35] L. S. Peak,[36] R. Pestotnik,[12] L. E. Piilonen,[44] H. Sahoo,[6] Y. Sakai,[7] O. Schneider,[16] J. Schümann,[7] C. Schwanda,[9] A. Sekiya,[21] K. Senyo,[20] M. Shapkin,[10] H. Shibuya,[37] J.-G. Shiu,[24] B. Shwartz,[1] S. Stanič,[28] M. Starič,[12] K. Sumisawa,[7] T. Sumiyoshi,[42] S. Suzuki,[32] M. Tanaka,[7] Y. Teramoto,[29] I. Tikhomirov,[11] K. Trabelsi,[7] Y. Uchida,[4] S. Uehara,[7] T. Uglov,[11] Y. Unno,[5] S. Uno,[7] P. Urquijo,[19] Y. Usov,[1] G. Varner,[6] K. E. Varvell,[36] K. Vervink,[16] C. C. Wang,[24] C. H. Wang,[23] M.-Z. Wang,[24] P. Wang,[8] X. L. Wang,[8] Y. Watanabe,[13] J. Wicht,[16] E. Won,[14] Y. Yamashita,[26] Z. P. Zhang,[33] V. Zhilich,[1] V. Zhulanov,[1] and A. Zupanc[12]

(The Belle Collaboration)

[1]*Budker Institute of Nuclear Physics, Novosibirsk*
[2]*Chiba University, Chiba*
[3]*University of Cincinnati, Cincinnati, Ohio 45221*
[4]*The Graduate University for Advanced Studies, Hayama*
[5]*Hanyang University, Seoul*
[6]*University of Hawaii, Honolulu, Hawaii 96822*
[7]*High Energy Accelerator Research Organization (KEK), Tsukuba*
[8]*Institute of High Energy Physics, Chinese Academy of Sciences, Beijing*
[9]*Institute of High Energy Physics, Vienna*
[10]*Institute of High Energy Physics, Protvino*
[11]*Institute for Theoretical and Experimental Physics, Moscow*
[12]*J. Stefan Institute, Ljubljana*
[13]*Kanagawa University, Yokohama*
[14]*Korea University, Seoul*
[15]*Kyungpook National University, Taegu*
[16]*École Polytechnique Fédérale de Lausanne (EPFL), Lausanne*
[17]*Faculty of Mathematics and Physics, University of Ljubljana, Ljubljana*
[18]*University of Maribor, Maribor*
[19]*University of Melbourne, School of Physics, Victoria 3010*
[20]*Nagoya University, Nagoya*
[21]*Nara Women's University, Nara*
[22]*National Central University, Chung-li*
[23]*National United University, Miao Li*
[24]*Department of Physics, National Taiwan University, Taipei*
[25]*H. Niewodniczanski Institute of Nuclear Physics, Krakow*
[26]*Nippon Dental University, Niigata*
[27]*Niigata University, Niigata*
[28]*University of Nova Gorica, Nova Gorica*
[29]*Osaka City University, Osaka*
[30]*Osaka University, Osaka*
[31]*Panjab University, Chandigarh*
[32]*Saga University, Saga*
[33]*University of Science and Technology of China, Hefei*
[34]*Seoul National University, Seoul*
[35]*Sungkyunkwan University, Suwon*

[36]University of Sydney, Sydney, New South Wales
[37]Toho University, Funabashi
[38]Tohoku Gakuin University, Tagajo
[39]Tohoku University, Sendai
[40]Department of Physics, University of Tokyo, Tokyo
[41]Tokyo Institute of Technology, Tokyo
[42]Tokyo Metropolitan University, Tokyo
[43]Tokyo University of Agriculture and Technology, Tokyo
[44]Virginia Polytechnic Institute and State University, Blacksburg, Virginia 24061
[45]Yonsei University, Seoul

(Received 4 April 2008; published 25 July 2008)

We report on a search for the doubly Cabibbo suppressed decay $B^+ \to D^{*+}\pi^0$, based on a data sample of 657×10^6 $B\bar{B}$ pairs collected at the $\Upsilon(4S)$ resonance with the Belle detector at the KEKB asymmetric-energy e^+e^- collider. We find no significant signal and set an upper limit of $\mathcal{B}(B^+ \to D^{*+}\pi^0) < 3.6 \times 10^{-6}$ at the 90% confidence level. This limit can be used to constrain the ratio between suppressed and favored $B \to D^*\pi$ decay amplitudes, $r < 0.051$, at the 90% confidence level.

DOI: 10.1103/PhysRevLett.101.041601 PACS numbers: 13.25.Hw, 11.30.Er, 12.15.Hh, 14.40.Nd

In the Standard Model, *CP* violation arises from a complex phase in the Cabibbo-Kobayashi-Maskawa (CKM) quark mixing matrix [1,2]. Precise measurements of CKM matrix parameters are therefore of fundamental importance for the description of the weak interaction of quarks and the investigation for the new sources of *CP* violation. Measurements of the time-dependent decay rates of $B^0(\bar{B}^0) \to D^{*\mp}\pi^\pm$ provide a theoretically clean method for extracting $\sin(2\phi_1 + \phi_3)$ [3], where ϕ_1 and ϕ_3 are the interior angles of the CKM triangle [4]. The *CP* violation parameters $S^\pm$ are given by [5]

$$S^\pm = \frac{2(-1)^L r \sin(2\phi_1 + \phi_3 \pm \delta)}{1 + r^2}, \quad (1)$$

where r is the ratio of the amplitudes of the doubly Cabibbo suppressed decay (DCSD), $B^0 \to D^{*+}\pi^-$ to the Cabibbo favored decay (CFD), $B^0 \to D^{*-}\pi^+$ (Fig. 1), L denotes the angular momentum of the final state, and δ is the strong phase difference between DCSD and CFD. It is difficult to determine r from B^0 decays because the DCSD amplitude is small compared to the contribution from mixing followed by CFD, $B^0 \to \bar{B}^0 \to D^{*+}\pi^-$.

Using available branching fraction measurements, r can be expressed as

$$r = \tan\theta_c \frac{f_{D^*}}{f_{D_s^*}} \sqrt{\frac{\mathcal{B}(B^0 \to D_s^{*+}\pi^-)}{\mathcal{B}(B^0 \to D^{*-}\pi^+)}}, \quad (2)$$

where θ_c is the Cabibbo angle, and the decay constants f_{D^*} and $f_{D_s^*}$ are available from lattice QCD calculations. However, the assumption of SU(3) symmetry and additional W-exchange contributions result in an uncertainty of about 30% on r. In order to avoid this uncertainty, one can instead use the isospin relation,

$$r = \sqrt{\frac{\tau_{B^0}}{\tau_{B^+}} \frac{2\mathcal{B}(B^+ \to D^{*+}\pi^0)}{\mathcal{B}(B^0 \to D^{*-}\pi^+)}}, \quad (3)$$

where $\tau_{B^+}/\tau_{B^0} = 1.071 \pm 0.009$ and $\mathcal{B}(B^0 \to D^{*-}\pi^+) = (2.76 \pm 0.21) \times 10^{-3}$ [6]. We naively estimate $\mathcal{B}(B^+ \to D^{*+}\pi^0) = 5.9 \times 10^{-7}$, taking into account the r factor of 0.02 calculated from Eq. (2) [7]. The previous search gives an upper limit of $\mathcal{B}(B^+ \to D^{*+}\pi^0) < 1.7 \times 10^{-4}$ at the 90% confidence level [8].

In this Letter, we report on a search for $B^+ \to D^{*+}\pi^0$ based on a data sample of 605 fb^{-1} corresponding to $(657 \pm 9) \times 10^6$ $B\bar{B}$ events, collected with the Belle detector [9] at the KEKB asymmetric-energy e^+e^- collider [10] operating at the $\Upsilon(4S)$ resonance.

The Belle detector is a large-solid-angle magnetic spectrometer that consists of a silicon vertex detector, a 50-layer central drift chamber (CDC), an array of aerogel threshold Cherenkov counters (ACC), a barrel-like arrangement of time-of-flight scintillation counters (TOF), and an electromagnetic calorimeter comprised of CsI(Tl) crystals located inside a superconducting solenoid coil that provides a magnetic field of 1.5 T. An iron flux-return located outside of the coil is instrumented to detect K_L^0 mesons and to identify muons.

To search for $B^+ \to D^{*+}\pi^0$, we reconstruct D^{*+} candidates by pairing a low momentum charged pion (π^+_{slow}) and a D^0, which is reconstructed through its decays to $K^-\pi^+$,

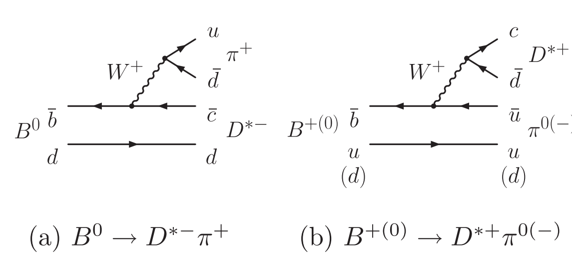

FIG. 1. Feynman tree diagrams for (a) CFD $B^0 \to D^{*-}\pi^+$ with the CKM coupling $V_{cb}^*V_{ud}$, and (b) DCSD $B^{+(0)} \to D^{*+}\pi^{0(-)}$ with the coupling $V_{ub}^*V_{cd}$.

$K^-\pi^+\pi^0$, $K^-\pi^+\pi^-\pi^+$, and $K_S^0\pi^+\pi^-$. Inclusion of charge conjugate modes is implied throughout this Letter.

For charged kaon and pion candidates except pions from K_S^0's, we require tracks to have a distance of closest approach to the interaction point within 5 cm along the z-axis (antiparallel to the positron beam direction) and within 2 cm in a plane perpendicular to the z-axis. Particle identification (PID) is based on the likelihoods $\mathcal{R}(K/\pi) = \mathcal{L}_K/(\mathcal{L}_K + \mathcal{L}_\pi)$, where $\mathcal{L}_K(\mathcal{L}_\pi)$ is the likelihood of kaons (pions) derived from the TOF, ACC, and dE/dx measurements in the CDC. The PID selections, which are $\mathcal{R}(K/\pi) > 0.3(<0.3)$ for kaons (pions) are applied to all charged particles except pions from K_S^0's. The PID efficiencies are 94% (91%) for kaons (pions), while the probability of misidentifying a pion as a kaon (a kaon as a pion) is 12% (6%).

Neutral pions are formed from photon pairs with an invariant mass between 0.118 GeV/c^2 and 0.150 GeV/c^2, corresponding to ± 3 standard deviations (σ). The photon momenta are then recalculated with a π^0 mass constraint. We require the π^0 momentum to be greater than 0.2 GeV/c in the center-of-mass system (c.m.s.), and the photon energy to be greater than 0.1 GeV in the laboratory frame.

K_S^0 candidates are reconstructed from pion pairs of oppositely-charged tracks with an invariant mass between 0.485 GeV/c^2 and 0.510 GeV/c^2, corresponding to $\pm 5\sigma$. Each candidate must have a displaced vertex with a flight direction consistent with that of a K_S^0 meson originating from the interaction point. Mass- and vertex-constrained fits are applied to obtain the 4-momenta of K_S^0 candidates.

For D^0 selection, the invariant mass of the daughter particles is required to be within 3σ from the nominal D^0 mass, where σ ($\sim$5 MeV/c^2) depends on the decay mode. D^{*+} candidates are required to have a mass difference $\Delta M = M_{D\pi} - M_D$ within 3σ from the nominal mass difference, where σ ($\sim$0.5 MeV/c^2) depends on the decay mode. Mass- and vertex-constrained fits are applied to D^0 and D^{*+} candidates.

We reconstruct a B^+ candidate from a D^{*+} and a π^0 candidate. We identify B decays based on requirements on the energy difference $\Delta E \equiv \sum_i E_i - E_{\rm beam}$ and the beam-energy constrained mass $M_{\rm bc} \equiv \sqrt{E_{\rm beam}^2 - |\sum_i \vec{p}_i|^2}$, where $E_{\rm beam}$ is the beam energy, and $\vec{p}_i$ and E_i are the momenta and energies of the daughters of the reconstructed B meson candidate, all in the c.m.s. We select candidates in a fit region defined as $|\Delta E| < 0.25$ GeV and 5.20 GeV/$c^2 < M_{\rm bc} < 5.29$ GeV/c^2. The signal region is defined as $|\Delta E| < 0.1$ GeV and 5.27 GeV/$c^2 < M_{\rm bc} < 5.29$ GeV/c^2.

To suppress the background from continuum ($e^+e^- \to q\bar{q}$, $q = u$, d, s, c) events, we calculate modified Fox-Wolfram moments [11] and combine them into a Fisher discriminant. We calculate a probability density function (PDF) for this discriminant and multiply it by PDFs for $\cos\theta_B$, Δz, and $\cos\theta_h$, where θ_B is the polar angle between the B direction and the beam direction in the c.m.s., Δz is the displacement along the beam axis between the signal B vertex and that of the other B, and θ_h is the angle between the $\pi^+_{\rm slow}$ direction and the opposite of the B momentum in the D^{*+} frame. The PDFs for signal, generic B events and continuum are obtained from GEANT3-based [12] Monte Carlo (MC) simulation. These PDFs are combined into a signal (background) likelihood variable $\mathcal{L}_{\rm sig(bkg)}$; we then impose requirements on the likelihood ratio $\mathcal{R} \equiv \mathcal{L}_{\rm sig}/(\mathcal{L}_{\rm sig} + \mathcal{L}_{\rm bkg})$. Additional background suppression is achieved through the use of a B-flavor tagging algorithm [13], which provides a discrete variable indicating the flavor of the tagging B meson and a quality parameter $r_{\rm tag}$, with continuous values ranging from 0 for no flavor information to unity for unambiguous flavor assignment. The backgrounds from continuum and generic B events are reduced by applying a selection requirement on $\mathcal{R}$ for events in each $r_{\rm tag}$ region that maximizes the value of $N_{\rm sig}/\sqrt{N_{\rm sig} + N_{\rm bkg}}$, where $N_{\rm sig}$ and $N_{\rm bkg}$ denote the expected signal and background yields in the signal region, based on MC simulation. This requirement eliminates 99% (94%) of the background from continuum (B decays) in the signal region, while retaining 35% of the signal.

The fraction of events with more than one candidate is 3%. We select the best $D^{*+}\pi^0$ candidate based on the value of $\chi^2_{\rm tot} = \chi^2_{M(D^0)} + \chi^2_{\Delta M} + \chi^2_{M(\pi^0)}$, where each χ^2 is defined as the squared ratio of the deviation of the measured parameter from the expected signal value and the corresponding resolution. The reconstruction efficiency is determined to be 0.56%, using the fitting procedure described below for the signal MC samples. The branching fractions of D^{*+} and D^0 are included in the efficiency [6].

After the selection criteria are applied, the dominant background sources in the fit region are the continuum events and $\bar{B}^0 \to D^{*+}\rho^-$, while other B decays such as $B^- \to D^0\rho^-$ and $\bar{B}^0 \to D^{*0}\pi^0$ have smaller contributions. To obtain the signal yield, we perform an unbinned two-dimensional (2D) extended-maximum-likelihood fit to the ΔE-$M_{\rm bc}$ distributions in the fit region. The likelihood function consists of the following components: signal, continuum background ($q\bar{q}$), $\bar{B}^0 \to D^{*+}\rho^-$, and other B decays.

The likelihood function for the signal is defined separately for each of the four D^0 decay modes and unified using the available branching fractions of the D^0 subdecays [6], while those for $q\bar{q}$ and backgrounds from B decays are defined as the sum of four D^0 decay modes. Each ΔE and $M_{\rm bc}$ shape for the signal is modeled by the sum of a Gaussian and a bifurcated Gaussian with means and widths fixed to the values obtained from MC simulation. The ΔE and $M_{\rm bc}$ PDFs for $q\bar{q}$ are modeled by a linear function and an ARGUS function [14], respectively. The backgrounds from $\bar{B}^0 \to D^{*+}\rho^-$ and other B decays are modeled by the superposition of Gaussian distributions constructed from unbinned MC events, where the width of each Gaussian represents the smoothing parameter for the event [15]. The $\bar{B}^0 \to D^{*+}\rho^-$ background forms a large peak in the region $\Delta E < -0.1$ GeV and $5.27\ \text{GeV}/c^2 < M_{bc} < 5.29\ \text{GeV}/c^2$. The size and shape of the $\bar{B}^0 \to D^{*+}\rho^-$ component strongly depend on the fraction of the longitudinal helicity component ($|H_0|$); we use $|H_0| = 0.941$ from Ref. [16].

The following parameters are allowed to vary: $q\bar{q}$ PDF parameters and yields of signal, $q\bar{q}$ and $\bar{B}^0 \to D^{*+}\rho^-$ components. The yield of other B decays is fixed to the branching fractions in Ref. [6].

Figure 2 shows the results of the fit to the data in the fit region. The projections of the fitted B signal in ΔE (M_{bc}) in the M_{bc} (ΔE) signal region are shown. We obtain $4.5^{+4.1}_{-3.4}$ $B^+ \to D^{*+}\pi^0$ signal candidates in the signal region (statistical error only). The significance is 1.4σ, defined by $\sqrt{-2\ln(\mathcal{L}_0/\mathcal{L}_{max})}$ where $\mathcal{L}_{max}$ ($\mathcal{L}_0$) is the likelihood value at the maximum (with the signal fixed to zero). The likelihood function is convolved with an asymmetric Gaussian distribution that represents the systematic error.

The systematic error components proportional to the signal yield are determined as follows. We estimate the systematic error from the $\mathcal{R}$ requirement by applying the $\mathcal{R}$ requirement to data and MC events using a $B^- \to D^0\rho^-$ control sample. The systematic error on the ΔM requirement is estimated by applying the ΔM requirement to $\bar{B}^0 \to D^{*+}\pi^-$ data and $B^+ \to D^{*+}\pi^0$ MC samples. The systematic error on the secondary branching fraction is calculated from errors given in Ref. [6]. The systematic error due to the charged-track reconstruction efficiency is estimated to be 1.0% (1.6%) per charged kaon (pion) using partially reconstructed D^{*+} events. The systematic error due to $\mathcal{R}(K/\pi)$ selection has a relative uncertainty of 0.8% (1.4%) per charged kaon (pion), determined from $D^{*+} \to D^0\pi^+$, $D^0 \to K^-\pi^+$ decays. The π^0 reconstruction is verified by comparing the ratio of $D^0 \to K^-\pi^+$ and $D^0 \to K^-\pi^+\pi^0$ yields with the MC expectation; an uncertainty of 3.0% per particle is assigned. The K_S^0 reconstruction is verified by comparing the ratio of $D^+ \to K_S^0\pi^+$ and $D^+ \to K^-\pi^+\pi^+$ yields with the MC expectation; an uncertainty of 4.9% is assigned. The systematic error due to the signal MC statistics is 0.5% and the error due to the uncertainty in the total number of $B\bar{B}$ pairs is 1.4%. The systematic error components proportional to the signal yield are summarized in Table I.

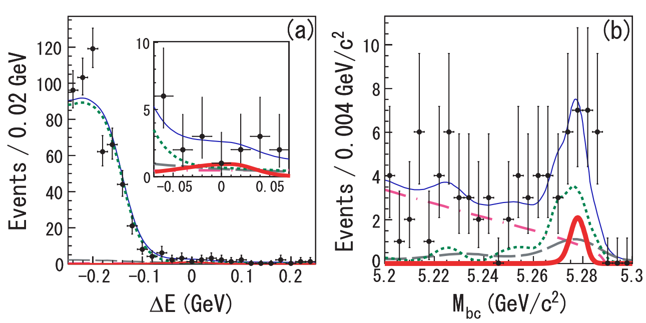

FIG. 2 (color online). Projections of the unbinned two-dimensional likelihood fit to data in the region $|\Delta E| < 0.25$ GeV and $5.20\ \text{GeV}/c^2 < M_{bc} < 5.29\ \text{GeV}/c^2$. (a) ΔE distribution for $5.27\ \text{GeV}/c^2 < M_{bc} < 5.29\ \text{GeV}/c^2$ with a magnified view of $|\Delta E| < 0.07$ GeV in the inset. (b) M_{bc} distribution for $|\Delta E| < 0.1$ GeV. The points with error bars represent the data, while the curves represent the various components from the fit: signal (thick solid line), continuum (dash-dotted line), $\bar{B}^0 \to D^{*+}\rho^-$ decay (dotted line), other B decays (dashed line), and the sum of all components (thin solid line).

The systematic errors on the yield extraction are estimated as follows. We estimate the uncertainty of $|H_0|$ of $\bar{B}^0 \to D^{*+}\rho^-$ by varying $|H_0|$ by $\pm1\sigma$, where the error of $|H_0|$ is taken from Ref. [16]. Possible ΔE shifts between data and MC simulation for the $\bar{B}^0 \to D^{*+}\rho^-$ background are evaluated by measuring the ΔE shift of the $B^- \to D^{*0}\rho^-$ background component using a $\bar{B}^0 \to D^{*0}\pi^0$ control sample. To obtain the systematic error on the background fraction of other B decays, we vary the normalizations of the individual sources by $\pm1\sigma$, where the values are taken from Ref. [6]. The normalization of other background components are varied by $\pm50\%$. The systematic error due to the uncertainty in the shape of the B background PDF is determined by varying the Gaussian smoothing width by factors of two and one half from its nominal value. Uncertainties from the two-dimensional correlation in the signal and the $q\bar{q}$ components are estimated by applying 2D background PDFs to the signal and the $q\bar{q}$ shapes. The effect of a possible bias in the fitting procedure is estimated by a toy MC study. The systematic errors on the yield extraction in the signal region are summarized in Table II.

We then obtain the branching fraction of $B^+ \to D^{*+}\pi^0$ to be $\mathcal{B}(B^+ \to D^{*+}\pi^0) = [1.2^{+1.1}_{-0.9}(\text{stat})^{+0.3}_{-0.9}(\text{syst})] \times 10^{-6}$.

The likelihood distribution ($\mathcal{L}$), which is convolved with the systematic error, is used to obtain the upper limit on the branching fraction. We calculate the 90% confidence level (C.L.) upper limit (UL) using the relation

TABLE I. Systematic errors for $\mathcal{B}(B^+ \to D^{*+}\pi^0)$, proportional to the signal yield.

Source	Systematic error (%) $\pm\sigma$
$\mathcal{R}$ requirement	3.0
ΔM requirement	3.3
Secondary branching fractions	3.3
Track finding efficiency	5.1
Particle identification	4.4
π^0 reconstruction	4.1
K_S^0 reconstruction	0.3
MC statistics	0.5
Number of $B\bar{B}$ pairs	1.4
Quadratic sum	9.8

TABLE II. Systematic errors for $\mathcal{B}(B^+ \to D^{*+}\pi^0)$, related to the yield extraction in the signal region.

Source	Systematic error (number of events) $+\sigma$	$-\sigma$
$\lvert H_0 \rvert$ of $\bar{B}^0 \to D^{*+}\rho^-$	0.7	-1.9
ΔE shift of $\bar{B}^0 \to D^{*+}\rho^-$	0.0	-0.6
Fraction of backgrounds	0.8	-0.4
Gaussian width of background PDF	0.5	-2.0
2D correlation for $q\bar{q}$ and $B^+ \to D^{*+}\pi^0$	0.0	-1.3
Fit bias	0.0	-0.5
Quadratic sum	1.2	-3.2

$\int_0^{\mathrm{UL}} \mathcal{L} d\mathcal{B} / \int_0^{\infty} \mathcal{L} d\mathcal{B} = 0.9$ to be

$$\mathcal{B}(B^+ \to D^{*+}\pi^0) < 3.6 \times 10^{-6}. \quad (4)$$

The obtained upper limit is consistent with the naive estimate, 5.9×10^{-7} discussed above. This result can be used to obtain an upper limit on the ratio of magnitudes of DCSD and CFD in $D^*\pi$ decay,

$$r < 0.051\,(90\%\ \mathrm{C.L.}). \quad (5)$$

To summarize, a search for the doubly Cabibbo suppressed decay $B^+ \to D^{*+}\pi^0$ in a data sample of 605 fb^{-1} yields an upper limit of $\mathcal{B}(B^+ \to D^{*+}\pi^0) < 3.6 \times 10^{-6}$ at the 90% confidence level. This limit can be used to constrain the ratio between suppressed and favored $B \to D^*\pi$ decay amplitudes, $r < 0.051$, at the 90% confidence level.

We thank the KEKB group for excellent operation of the accelerator, the KEK cryogenics group for efficient solenoid operations, and the KEK computer group and the NII for valuable computing and SINET3 network support. We acknowledge support from MEXT and JSPS (Japan); ARC and DEST (Australia); NSFC (China); DST (India); MOEHRD, KOSEF and KRF (Korea); KBN (Poland); MES and RFAAE (Russia); ARRS (Slovenia); SNSF (Switzerland); NSC and MOE (Taiwan); and DOE (USA).

[1] N. Cabibbo, Phys. Rev. Lett. **10**, 531 (1963).
[2] M. Kobayashi and T. Maskawa, Prog. Theor. Phys. **49**, 652 (1973).
[3] I. Dunietz and R. G. Sachs, Phys. Rev. D **37**, 3186 (1988); **39**, 3515(E) (1989); I. Dunietz, Phys. Lett. B **427**, 179 (1998).
[4] The angles ϕ_1 and ϕ_3 are also sometimes known as β and γ, respectively.
[5] R. Fleischer, Nucl. Phys. B **671**, 459 (2003).
[6] Y.-M. Yao *et al.* (Particle Data Group), J. Phys. G **33**, 1 (2006).
[7] F. J. Ronga and T. R. Sarangi *et al.* (Belle Collaboration), Phys. Rev. D **73**, 092003 (2006).
[8] G. Brandenburg *et al.* (CLEO Collaboration), Phys. Rev. Lett. **80**, 2762 (1998).
[9] A. Abashian *et al.* (Belle Collaboration), Nucl. Instrum. Methods Phys. Res., Sect. A **479**, 117 (2002).
[10] S. Kurokawa and E. Kikutani, Nucl. Instrum. Methods Phys. Res., Sect. A **499**, 1 (2003), and other papers included in this volume.
[11] G. C. Fox and S. Wolfram, Phys. Rev. Lett. **41**, 1581 (1978); The modified moments used in this Letter are described in S. H. Lee *et al.* (Belle Collaboration), Phys. Rev. Lett. **91**, 261801 (2003).
[12] R. Brun *et al.*, CERN Report No. DD/EE/84-1 (1984), GEANT 3.21.
[13] H. Kakuno *et al.*, Nucl. Instrum. Methods Phys. Res., Sect. A **533**, 516 (2004).
[14] H. Albrecht *et al.* (ARGUS Collaboration), Phys. Lett. B **241**, 278 (1990).
[15] K. Cranmer, Comput. Phys. Commun. **136**, 198 (2001).
[16] S. E. Csorna *et al.* (CLEO Collaboration), Phys. Rev. D **67**, 112002 (2003).